

Chemical Switching of Magnetic Properties through Topotactic Lithium Exchange in Manganese(III) Arsenate Hydrate

Miguel A. G. Aranda,^{* a,b} J. Paul Attfield,^b Sebastian Bruque^a and R. B. Von Dreele^c

^a Departamento de Química Inorgánica, Universidad de Málaga, Aptd. 59, 29071 Málaga, Spain

^b Department of Chemistry, University of Cambridge, Lensfield Road, Cambridge, UK CB2 1EW

^c LANSCE, Los Alamos National Laboratory, Los Alamos, New Mexico, 87545, USA

The switch in local Jahn–Teller distortions of the $\text{Mn}^{\text{III}}\text{O}_6$ octahedra caused by the topotactic ion-exchange reaction of $\text{MnAsO}_4 \cdot \text{H}_2\text{O}$ to give $\text{LiMnAsO}_4(\text{OH})$ results in a novel switch from antiferromagnetic to ferromagnetic order within infinite Mn–O–Mn chains in the framework, although in both materials the overall order is antiferromagnetic.

Phosphates and arsenates of the first-row transition metals exhibit a wide range of interesting chemical and physical properties such as ion exchange and conduction, catalysis, non-linear optical properties and magnetic order. As part of a study of manganese phosphates and arsenates, we have shown previously that $\text{MnAsO}_4 \cdot \text{H}_2\text{O}$ undergoes a lithium exchange reaction with solid LiNO_3 to give $\text{LiMnAsO}_4(\text{OH})$.¹ This reaction is accompanied by an unusual switch in the framework geometry as the Jahn–Teller distortions of the MnO_6 octahedra change, although the topology is unaltered. This distortion might result in a change in the magnetic interactions, so we have determined the low temperature magnetic structures of both compounds. The antiferromagnetic structure $\text{MnAsO}_4 \cdot \text{D}_2\text{O}$ at 4 K has been reported elsewhere;² in this communication we present the magnetic structure of $\text{LiMnAsO}_4(\text{OH})$ and show that a switch in magnetic properties does occur.

Polycrystalline LiNO_3 and $\text{MnAsO}_4 \cdot \text{D}_2\text{O}$ were ground in a 2 : 1 molar ratio and heated at 200 °C for 3 weeks under flowing N_2 . The reaction mixture was washed with D_2SO_4 – D_2O and D_2O , and dried at 60 °C. Powder X-ray diffraction showed that the product was highly crystalline, single phase, $\text{LiMnAsO}_4(\text{OD})$. Time-of-flight neutron powder diffraction patterns were collected on instrument HIPD at LANSCE, Los Alamos National Laboratory, USA at room temp. and 10 K. The data were normalised to the incident beam spectrum and fitted by the Rietveld method³ using the GSAS package.⁴ Simultaneous refinements of the six spectra from counter banks at ± 153 , ± 90 and $\pm 40^\circ 2\theta$ were performed using a Gaussian convoluted with a double exponential peak shape function,⁵ and a refined Fourier series background function. Neutron scattering lengths were taken from Koster and Yelon⁶ and the free ion form factor of Freeman and Watson⁷ was used to calculate the magnetic intensities.

Rietveld refinements using the room temp. and 10 K neutron diffraction data confirm the structure of $\text{LiMnAsO}_4(\text{OD})$, including the Li position, and a difference Fourier map revealed the D atom.⁸ Magnetic diffraction peaks were clearly observed in the 10 K pattern and could be indexed upon the C-centred setting of the triclinic nuclear unit cell with reflection conditions shown in Table 1. As the Mn atoms lie on special crystallographic positions, these conditions are sufficient to define the relative orientations of the four Mn spins. A good fit to the magnetic intensities was obtained (average magnetic $R_F = 4.3\%$ for $\pm 40^\circ 2\theta$ data sets) by refining this colinear model with magnetic components parallel to all three axes. The parameters for $\text{LiMnAsO}_4(\text{OD})$ are compared to those of $\text{MnAsO}_4 \cdot \text{D}_2\text{O}$ in Table 1.[†]

Both $\text{MnAsO}_4 \cdot \text{D}_2\text{O}$ and $\text{LiMnAsO}_4(\text{OD})$ order antiferromagnetically with Neel temperatures of 24 and 30 K, respectively,⁸ but neutron diffraction shows that the moments are arranged differently in the two antiferromagnetic phases (Fig. 1). In $\text{MnAsO}_4 \cdot \text{D}_2\text{O}$ the spins are antiferromagnetically coupled within infinite chains of corner sharing octahedra that are parallel to [101], whereas in $\text{LiMnAsO}_4(\text{OD})$ ferromagnetic spin chains are present. In both cases, neighbouring spin chains are antiferromagnetically coupled, giving rise to overall antiferromagnetic behaviour. The magnetic moments do not

differ significantly in magnitude, being reduced by $0.5 \mu_B$ from the free-ion value ($4 \mu_B$) due to Mn–O covalency,⁹ and lie along [101] in $\text{MnAsO}_4 \cdot \text{D}_2\text{O}$ but are almost perpendicular [$82(2)^\circ$] to this direction in $\text{LiMnAsO}_4(\text{OD})$.

The switch in the magnetic intrachain interaction and easy axis upon exchange of Li^+ for H^+ in $\text{MnAsO}_4 \cdot \text{H}_2\text{O}$ is consistent with the switch in framework geometry described

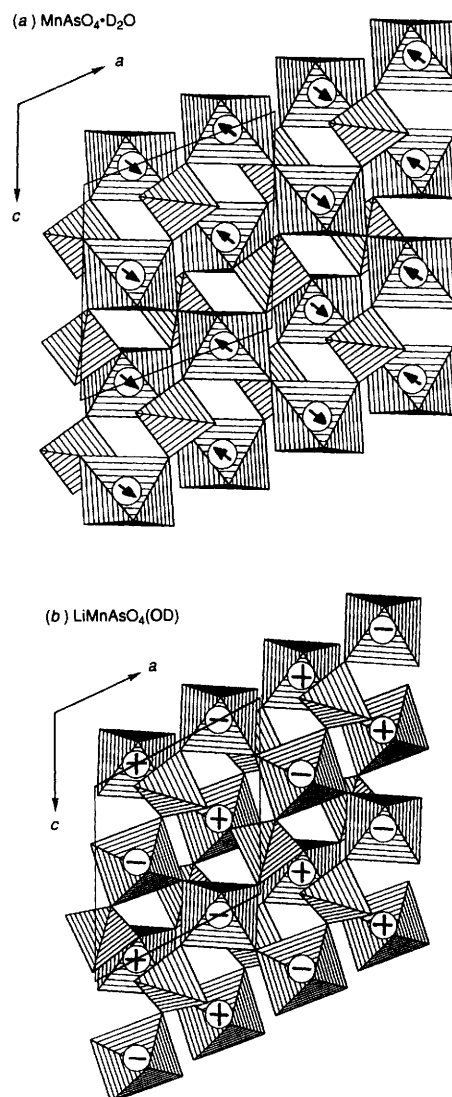


Fig. 1 Polyhedral views of (a) $\text{MnAsO}_4 \cdot \text{D}_2\text{O}$, and (b) $\text{LiMnAsO}_4(\text{OD})$ with the magnetic structures shown. In (a) the moments lie in the ac plane and are coupled antiferromagnetically within chains of linked octahedra parallel to [101], whereas in (b) the moments are coupled ferromagnetically within the chains and are near-perpendicular to the ac plane.

Table 1 Geometric and magnetic parameters for $\text{MnAsO}_4 \cdot \text{D}_2\text{O}$ at 4 K² and $\text{LiMnAsO}_4(\text{OD})$ at 10 K, with estimated standard deviations in parentheses

	$\text{MnAsO}_4 \cdot \text{D}_2\text{O}$	$\text{LiMnAsO}_4(\text{OD})^a$
Bond distances (Å)	Mn–O(1) 1.863(1)	Mn(a)–O(1a) 1.836(2) Mn(b)–O(1b) 1.919(1)
	Mn–O(2) 1.861(1)	Mn(a)–O(2b) 2.179(1) Mn(b)–O(2a) 2.214(1)
	Mn–O(3) 2.255(1)	Mn(a)–O(3) 2.001(2) Mn(b)–O(3) 1.973(2)
Bridging angle (°)	Mn–O(3)–Mn 122.7(1)	Mn(a)–O(3)–Mn(b) 132.2(1)
Magnetic reflection conditions $h + k, h + l, k + l$	odd, odd, even	odd, even, odd
Relative Mn spin directions $\frac{1}{4} \frac{1}{4} 0, \frac{3}{4} \frac{3}{4} 0, \frac{3}{4} \frac{1}{4} \frac{1}{2}, \frac{1}{4} \frac{3}{4} \frac{1}{2}$	+, -, -, +	+ (a), - (a), + (b), - (b)
Magnetic moment components ^b μ_a, μ_b, μ_c (μ_B)	3.12(4), 0.0, 3.23(4)	0.72(4), 3.38(5), 0.33(5)
Resultant moment (μ_B)	3.54(5)	3.48(5)

^a Inequivalent atoms a and b in $\text{LiMnAsO}_4(\text{OD})$ are symmetry equivalent in $\text{MnAsO}_4 \cdot \text{D}_2\text{O}$. ^b Parallel to the cell vectors.

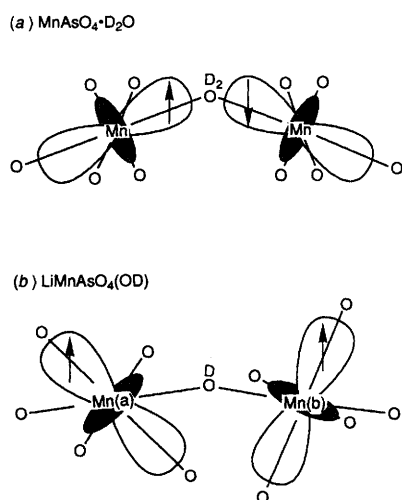


Fig. 2 Schematic views of Jahn–Teller distorted octahedra linked through (a) D_2O in $\text{MnAsO}_4 \cdot \text{D}_2\text{O}$, and (b) OD^- in $\text{LiMnAsO}_4(\text{OD})$ with the $d_{3/2}$ orbitals and relative spin directions shown

previously.¹ Octahedrally coordinated, high spin, $3d^4 \text{Mn}^{3+}$ is subject to a $[4 + 2]$ Jahn–Teller distortion, resulting in the electronic configuration $3d_{xy}^1 3d_{xz}^1 3d_{yz}^1 3d_{z^2}^1$ with elongation along the local z axis. In $\text{MnAsO}_4 \cdot \text{H}_2\text{O}$ the long Mn–O(3) bonds are those to the water molecules that bridge the octahedra (Table 1) into infinite chains. The $3d_{z^2}$ orbitals containing unpaired electrons on adjacent cations are thus directed towards the bridging oxygen atom, enabling σ -overlap to give rise to a strong, antiferromagnetic, kinetic exchange interaction for the 123° bridging angle, as shown in Fig. 2(a).

The topotactic formation of $\text{LiMnAsO}_4(\text{OH})$ results in a deprotonation of the water molecules bridging adjacent Mn^{3+} cations, which become crystallographically inequivalent due to the lowering of symmetry from monoclinic to triclinic. The increased negative charge on the bridging hydroxide groups results in the switch of local Jahn–Teller modes, so that the long Mn–O bonds associated with the $3d_{z^2}$ orbitals are now to non-bridging arsenate oxygens O(2a) and O(2b) (Table 1). σ -superexchange through the Mn(a)–O(3)–Mn(b) bridge is no longer possible [Fig. 2(b)], but weaker π -superexchange could occur through the overlap of half-filled Mn: $3d_{xy}$ and $3d_{xz}$ or $3d_{yz}$ orbitals with O: $2p_\pi$ lobes. However, as the Mn(a)O₆ and Mn(b)O₆ octahedra are rotated by differing amounts out of the Mn(a)–O(3)–Mn(b) plane [the angles between the Mn(a)–O(2b) and Mn(b)–O(2a) bonds and this plane are $45.6(1)$ and $23.6(1)^\circ$, respectively], the π -symmetry Mn(a) and Mn(b) $3d$

orbitals are effectively orthogonal, and ferromagnetic potential exchange results.

Thus, the chemical switching of Mn^{3+} Jahn–Teller modes caused by the deprotonation of $\text{MnAsO}_4 \cdot \text{H}_2\text{O}$ in forming $\text{LiMnAsO}_4(\text{OH})$ results in a magnetic switch from antiferromagnetic to ferromagnetic superexchange within the chains of corner linked MnO_6 octahedra. The ordering between chains is antiferromagnetic in both cases. ‘*Chimie douce*’ has been used previously to alter the magnitude of magnetic properties, for example, the Curie temperature of electrochemically intercalated $\text{Cu}_{1+y}\text{Cr}_2\text{Se}_4$ spinels varies from 432 K ($y = 0$) to 175 K ($y = 1$).¹⁰ However, the switch in sign of the Mn–O–Mn superexchange interaction and hence the overall magnetic structure in the $\text{MnAsO}_4 \cdot \text{H}_2\text{O}$ framework is a novel result in ion-exchange chemistry.

M. A. G. A. acknowledges the Spanish Government for financial support and the EC for a Human Capital and Mobility Fellowship. LANSCE is operated under US Government Contract W-7405-ENG-36.

Received, 29th June 1993; Com. 3/03704E

Footnote

[†] $\text{MnAsO}_4 \cdot \text{D}_2\text{O}$ is monoclinic $C2/c$, 4 K cell parameters are $a = 6.8707(3)$, $b = 7.6958(3)$, $c = 7.3121(3)$ Å, $\beta = 112.221(2)^\circ$; $\text{LiMnAsO}_4(\text{OD})$ is triclinic, 10 K cell parameters in the $C\bar{1}$ setting are $a = 6.8760(2)$, $b = 8.4147(3)$, $c = 7.2421(3)$ Å, $\alpha = 94.320(2)$, $\beta = 118.114(2)$, $\gamma = 86.474(2)^\circ$.

References

- M. A. G. Aranda, J. P. Attfield and S. Bruque, *J. Chem. Soc., Chem. Commun.*, 1991, 604.
- M. A. G. Aranda, J. P. Attfield, S. Bruque and F. Palacio, *J. Mater. Chem.*, 1992, 2, 501.
- H. M. Rietveld, *J. Appl. Crystallogr.*, 1969, 2, 65.
- A. C. Larson and R. B. Von Dreele, Los Alamos National Laboratory Report No. LA-UR-86-748, 1987.
- R. B. Von Dreele, J. D. Jorgensen and C. G. Windsor, *J. Appl. Crystallogr.*, 1982, 15, 581.
- L. Koster and W. B. Yelon, *Summary of low energy neutron scattering wavelengths and cross sections*, Netherland Energy Research Foundation, Department of Physics, Petten, 1982.
- A. J. Freeman and R. E. Watson, *Acta Crystallogr.*, 1961, 14, 231.
- M. A. G. Aranda, J. P. Attfield, S. Bruque, F. Palacio and R. B. Von Dreele, manuscript in preparation.
- B. C. Tofield, *The Study of Covalency by Magnetic Neutron Scattering*, Springer-Verlag, Berlin, Heidelberg, 1975.
- R. Schöllhorn and A. Payer, *Angew. Chem., Int. Ed. Engl.*, 1986, 25, 905.